Measurement of time-integrated untagged decay rate asymmetry in semileptonic B_s decays

DØ Collaboration
(Dated: 14 June 2006)

We performed a first direct measurement of the untagged decay rate asymmetry in semileptonic B_s decays, A^s_{SL}, using an untagged sample of $B^0_s \to D^-_s \mu^+ \nu X$ decays, where $D^-_s \to \phi\pi^-$, $\phi \to K^+K^-$. This sample was selected from $1 fb^{-1}$ of data collected by the Tevatron from April 2002 to January 2006. We obtained $A^s_{SL} = [2.45 \pm 1.93(\text{stat}) \pm 0.35(\text{syst})] \times 10^{-2}$. This result is to be compared with SM prediction $A^s_{SL} = (0.21 \pm 0.04) \times 10^{-4}$ which in the presence of New Physics can be enhanced up to 0.5×10^{-2}.

I. MOTIVATION

At present, one of the principal measurements in B physics is the measurement of untagged decay rate asymmetry in semileptonic B_s transitions, referred to hereafter as the semileptonic decay rate asymmetry, A^s_{SL}. A measurement of A^s_{SL} is an important test of possible new physics contributions to mixing amplitude M_s, which in the most general way is parametrised as follows [1]:

$$M_s = r_s^2 e^{2i\theta_s} M_s^{\rm SM}, \tag{1}$$

where $M_s^{\rm SM}$ is the Standard Model contribution to the mixing amplitude. A^s_{SL} is important for constraining $\sin 2\theta_s$ [1]. According to [2] the time evolution of the semileptonic decay rate asymmetry from an untagged sample, $A^s_{SL,unt}(t)$ is related to the measure of CP violation in mixing,

$$a = {\rm Im}\,\frac{\Gamma_s}{M_s}, \tag{2}$$

in the following way:

$$A^s_{SL,unt}(t) \; = \; \frac{\Gamma[f,t]-\Gamma[\overline{f},t]}{\Gamma[f,t]+\Gamma[\overline{f},t]} \; = \; \frac{a}{2} - \frac{a}{2}\,\frac{\cos(\Delta M_s\, t)}{\cosh(\Delta\Gamma_s t/2)}. \tag{3}$$

Here $\Gamma[f,t]$ and $\Gamma[\overline{f},t]$ are untagged decay rates, and ΔM_s and $\Delta\Gamma_s$ are the mass and width differences between neutral B_s states.

The time integral of (3) does not vanish due to constant term $\frac{a}{2}$:

$$A^{s,int}_{SL,unt} \; \equiv \; \frac{\int_0^\infty dt[\Gamma[f,t]-\Gamma[\overline{f},t]]}{\int_0^\infty dt[\Gamma[f,t]+\Gamma[\overline{f},t]]} \; = \; \frac{a}{2}\,\frac{x_s^2-y_s^2}{x_s^2+1} \; \approx \; \frac{a}{2}, \tag{4}$$

Here $x_s = \Delta M_s/\Gamma_s$, $y_s = \Delta\Gamma_s/(2\Gamma_s)$ as usual.

In [3] it has been shown that the wrong-sign semileptonic decay rate asymmetry measured on a tagged sample is

$$A_{SL} = a + \mathcal{O}(a^2), \tag{5}$$

so an untagged sample can still be used to measure semileptonic decay rate asymmetry, taking into account

$$A^s_{SL} = 2A^{s,int}_{SL,unt}. \tag{6}$$

Experimentally, $A^{s,int}_{SL,unt}$ is equal to an integrated charge asymmetry between decays of B_s to f and $\overline{f}$:

$$A^{s,int}_{SL,unt} = \frac{N_+ - N_-}{N_+ + N_-}, \tag{7}$$

N_+ is the number of decays to f, whilst N_- is the number of decays to $\overline{f}$, $f = Xl^+\nu_l$.

Standard Model predicts [2]

$$A^s_{SL} = (0.21 \pm 0.04) \times 10^{-4} \tag{8}$$

In the presence of New Physics this value can be enhanced up to 0.5×10^{-2} which corresponds to $\sin 2\theta_s \sim 1$ in (1), see [4].

II. DETECTOR DESCRIPTION

The DØ detector is described in detail elsewhere [5]. The following elements of the detector are essential for this analysis:

- The magnetic central-tracking system, which consists of a silicon microstrip tracker (SMT) and a central fiber tracker (CFT), both located within a 2-T superconducting solenoidal magnet;
- The muon system located beyond the calorimeter which consists of proportional drift tubes (PDTs), toroidal magnets, central scintillation counters, and a forward muon system.

III. EVENT SELECTION

We measured the integrated charge asymmetry in a $B_s^0 \to D_s^- \mu^+ \nu X$, $D_s^- \to \phi\pi^-$, $\phi \to K^+K^-$ data sample selected from $1 fb^{-1}$ of data taken from April 2002 to January 2006. Charge conjugate states are assumed throughout this paper. The selections are described in detail in [10]. Three tracks with $p_T > 15$ GeV/c and a good muon were selected. The D_s^- candidate was constructed from three tracks included in same jet as the reconstructed muon. Two oppositely charged tracks were assigned a kaon mass and were combined to a ϕ satisfying $1.004 < M(K^+K^-) < 1.034$ GeV/c^2. The third track was assigned a pion mass and was required to have a charge opposite to that of the muon: $q_\mu \cdot q_\pi < 0$.

In addition we used a cut on the *visible proper decay length* (VPDL) of B_s^0: VPDL(B_s^0)> 0. VPDL is defined as follows:

$$\text{VPDL} = \frac{\overline{d_T^B} \cdot \overline{p_T^{\mu D_s}}}{(p_T^{\mu D_s})^2} \cdot c M_B.$$

Here $\overline{d_T^B}$ is a transverse projection of the impact parameter of the reconstructed B meson, $\overline{p_T^{\mu D_s}}$ is a transverse momentum of μD_s system, M_B is the B meson mass, as reported by PDG [11]. This cut reduces the contribution from c-$\bar{c} \to D_s^- \mu^+ \nu X$ events since they have a VPDL distribution with zero mean and $\sigma \sim 150 \mu m$ [12].

The invariant mass distribution $M(K^+K^-\pi^-)$ is shown on Fig. 1. The left and right peaks correspond to $\mu^+ D^-$ and $\mu^+ D_s^-$ candidates, respectively. The curve represents the fit function to the $M(KK\pi)$ spectrum. For fitting the mass spectra, a single Gaussian was used to describe $D^- \to \phi\pi^-$, a double Gaussian - to describe $D_s^- \to \phi\pi^-$, whilst background was modelled by an exponential. The total number of D_s^- events passing all cuts in the mass peak is $27,275 \pm 296$.

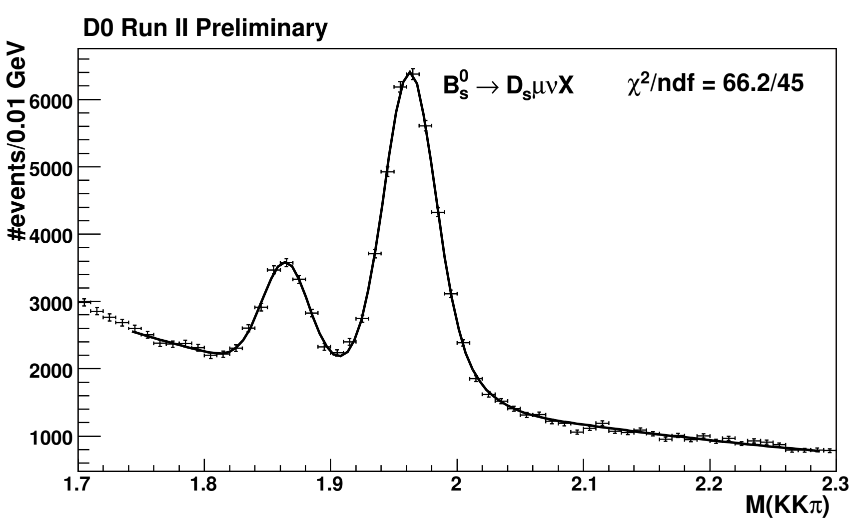

FIG. 1: $M(KK\pi)$ invariant mass distribution for the untagged B_s^0 sample.

TABLE I: The number of events in the signal D_s^- mass peak and background normalisation for $\beta\gamma q$-th sample.

Subsample: $\beta\gamma q$	$n_q^{\beta\gamma}$ (signal, # of evts)	$n_q^{\beta\gamma}$ (bckg normalisation, arbitrary units)
$+++$	3,216 ± 76	1,370 ± 17
$+-+$	3,586 ± 79	1,452 ± 18
$++-$	3,391 ± 78	1,453 ± 18
$+--$	3,225 ± 76	1,375 ± 17
$-++$	3,616 ± 80	1,469 ± 18
$--+$	3,370 ± 77	1,397 ± 17
$-+-$	3,353 ± 77	1,429 ± 18
$---$	3,532 ± 79	1,496 ± 18

IV. ANALYSIS METHOD

To extract physics and detector asymmetries we divided the sample into 8 subsamples corresponding to 8 possible combinations of toroid polarity β, sign of pseudorapidity γ ($\gamma = +1$ if $\eta > 0$ and $\gamma = -1$ if $\eta < 0$) and muon charge q.

The $M(KK\pi)$ spectra of all samples are shown on Fig. 3. We fitted these distributions using the sum of a single Gaussian to describe D^- mass peak, a double Gaussian to describe D_s^- mass peak, and an exponential to describe the background. During the fitting procedure the mass peak widths, positions, the fraction of a "second" Gaussian in the D_s^- mass peak, as well as the background slope were fixed to the values defined from the fit to a $M(KK\pi)$ distribution of the undivided sample. We determined the number of events in a D_s^- peak of each $\beta\gamma q$-th sample, $n_q^{\beta\gamma}$. These numbers are shown in Table I, along with the background normalisation in arbitrary units.

The set of 8 $n_q^{\beta\gamma}$ numbers was used to disentangle the muon charge asymmetry from other possible physics and detector asymmetries. We did this according to a parametrisation proposed in [13]. Let $n_q^{\beta\gamma}$ be the number events containing muons and passing the offline filter, where $q = \pm 1$ is the muon charge, $\beta = \pm 1$ is the toroid polarity and $\gamma = \pm 1$ is sign of pseudorapidity. Then, the physics and the detector can be modelled as follows:

$$\begin{aligned} n_q^{\beta\gamma} &= \frac{1}{4} N \epsilon^\beta (1 + qA)(1 + q\gamma A_{fb})(1 + \gamma A_{det})(1 + q\beta\gamma A_{ro}) \\ &\quad \times (1 + \beta\gamma A_{\beta\gamma})(1 + q\beta A_{q\beta}) \end{aligned} \tag{9}$$

where N is the number of signal events in the sample; ϵ^β is the fraction of integrated luminosity with toroid polarity β ($\epsilon^+ + \epsilon^- = 1$); A is the integrated charge asymmetry to be measured; A_{fb} is the forward-backward asymmetry of the detector (which accounts for the fact that more muons may go in proton direction); A_{det} is the north-south asymmetry of the detector (if any); A_{ro} is the range-out asymmetry which accounts for the decrease of acceptance of muons which bend towards toroid. $A_{\beta\gamma}$ and $A_{q\beta}$ are added to complete the system.

The system of 8 simultaneous equations (9) was solved using the MINUIT program [14] to extract all the asymmetries. Results are presented in Table II. Results for an exponentially modelled background are shown for comparison. Note, that the physics asymmetries (A and A_{fb}) for background are consistent with zero. Only the range-out asymmetry, A_{ro} is considerable and the same (within 1σ) both for signal and background. This shows the consistency of the method.

The numbers of events in the D^- mass peak of 8 subsamples and the asymmetries are shown in the Tables III and IV as a cross-check. Note that the errors are much bigger due to reduced statistics.

V. SAMPLE COMPOSITION

The contribution to the $D_s\mu$ signal from various processes is calculated in [6] from PDG branching fractions or EvtGen [9] inputs for branching fractions not given in PDG. In addition the contribution from c-$\bar{c} \to D_s^- \mu^+ \nu X$ was taken into account. According to [7] for the untagged sample it comprises 11.8 ± 3.4 % before the VPDL> 0 cut. Assuming that the VPDL cut rejects half of it we recalculated all contributions. The results are shown in Table V.

$B \to D_{(s)}^+ D_s^- X$ followed by $D_{(s)}^+ \to \mu^+ \nu X$ do not have flavor information and hence are not included in the signal contribution. The total contribution from signal (the first five channels) is $83.2 \pm 3.3\%$.

TABLE II: The time-integrated muon charge asymmetry from the D_s^- mass peak measured on an untagged sample is marked out in bold.

par	*signal*	*background*
N	$27,289 \pm 220$	$11,441 \pm 50$
ϵ^+	0.4916 ± 0.0040	0.4938 ± 0.0022
$\boldsymbol{A}$	**0.01021 ± 0.00806**	-0.00557 ± 0.00445
A_{fb}	-0.00459 ± 0.00806	-0.00203 ± 0.00428
A_{det}	-0.00511 ± 0.00806	0.00014 ± 0.00437
A_{ro}	-0.03517 ± 0.00805	-0.02634 ± 0.00439
A_{bg}	-0.00965 ± 0.00806	-0.00096 ± 0.00440
A_{ab}	0.00304 ± 0.00806	0.00464 ± 0.00439

TABLE III: Cross-check: the number of events in the D^- mass peak for $\beta\gamma q$-th sample.

Subsample: $\beta\gamma q$	$n_q^{\beta\gamma}$ (signal, # of evts)	$n_q^{\beta\gamma}$ (bckg normalisation, arbitrary units)
$+++$	907 ± 55	1,370 ± 17
$+-+$	965 ± 56	1,452 ± 18
$++-$	1,037 ± 57	1,453 ± 18
$+--$	963 ± 55	1,375 ± 17
$-++$	1,003 ± 57	1,469 ± 18
$--+$	801 ± 54	1,397 ± 17
$-+-$	831 ± 55	1,429 ± 18
$---$	1,116 ± 59	1,496 ± 18

TABLE IV: Cross-check: muon charge asymmetry from the D^- mass peak.

par	*signal*	*background*
N	$7,623 \pm 162$	$11,441 \pm 50$
ϵ^+	0.5100 ± 0.0106	0.4938 ± 0.0022
A	-0.03454 ± 0.02105	-0.00557 ± 0.00445
A_{fb}	0.04803 ± 0.02101	-0.00203 ± 0.00428
A_{det}	-0.00720 ± 0.02122	0.00014 ± 0.00437
A_{ro}	-0.08188 ± 0.02087	-0.02634 ± 0.00439
A_{bg}	0.01037 ± 0.02129	-0.00096 ± 0.00440
A_{ab}	0.00145 ± 0.02124	0.00464 ± 0.00439

At a hadron collider both B_d and B_s contribute to the measured muon charge asymmetry [8]:

$$A_{SL,measured} = k_d A_{SL}^d + k_s A_{SL}^s,$$

where k_d and k_s are fractions of the B_d and B_s decay modes correspondingly.

However, the B_d contribution to $A_{SL,measured}$ is small due to:

1. smallness of A_{SL}^d [2], the experimental world average is [11] $A_{SL}^d = 0.002 \pm 0.013$;
2. small B_d content in the sample: time-integrated A_{SL}^d component may result only from 3.9% of B^0 decay mode, see Table V.

To take the sample composition into account we divide the charge asymmetry from Table II by signal contribution $k_s = 83.2 \pm 3.3\%$ from flavor-preserving B_s channels and account for A_{SL}^d contamination as a systematic error (see the corresponding section).

According to (6) the semileptonic decay rate asymmetry is twice the corrected charge asymmetry. The final result is $A_{SL}^s = [2.45 \pm 1.93(\text{stat})] \times 10^{-2}$.

TABLE V: $D_s\mu$ sample composition.

Process	%
$B_s^0 \to \mu^+\nu D_s^-$	20.5 ± 1.2
$B_s^0 \to \mu^+\nu D_s^{-*} \to \mu^+\nu D_s^- X$	57.3 ± 3.2
$B_s^0 \to \mu^+\nu D_{s0}^{-*} \to \mu^+\nu D_s^- X$	1.3 ± 0.5
$B_s^0 \to \mu^+\nu D_{s1}^{\prime -} \to \mu^+\nu D_s^- X$	2.9 ± 0.5
$B_s^0 \to \tau^+\nu D_s^- \to \mu^+\nu D_s^- X$	1.2 ± 0.5
$B_s^0 \to D_s^+ D_s^- X; D_s^- \to \mu\nu X$	$2.7^{+1.1}_{-2.1}$
$B_s^0 \to D D_s X; D \to \mu\nu X$	0.8 ± 0.5
$B^+ \to D^+ D_s^- X; D \to \mu\nu X$	3.8 ± 1.3
$B^0 \to D^+ D_s^- X; D \to \mu\nu X$	3.9 ± 1.4
$c\text{-}\bar{c} \to D_s^- \mu^+\nu X$	5.6 ± 3.4

VI. SYSTEMATIC ERRORS

The following potential sources of systematic errors were considered and rejected:

- From [11] we learn that $c/\bar{c} \to K^{-/+}$ is charge symmetric and cannot produce muon charge asymmetry due to $K^\pm \to \mu^\pm$. However, $K^\pm \to \mu^\pm$ itself turns out to be charge asymmetric due to the asymmetric inelastic interaction cross-section of K^+ and K^- in the calorimeter: $\sigma(K^- d) > \sigma(K^+ d)$, see [13]. Hence, K^+-s last longer and can produce more μ^+-s. In [13] the corresponding single muon charge asymmetry is estimated to be 0.026 ± 0.005. However as long as K-s enter each decay in pairs, the reconstruction of D_s^+ and D_s^- remains charge symmetric and does not produce any systematic error.
- To select signal events we reconstruct μ and D_s by its decay to $\phi\pi^-$ in the final state. But μ may come from K in the decay chain of b quark and induce muon charge asymmetry due to the charge asymmetric $K^\pm \to \mu^\pm$ decay mentioned above, see Fig. 2. However, since such "incorrect" muons come from Cabbibo-allowed $c \to s$ transitions it has the same charge as the pion of the D_s signature. We suppress this source of charge asymmetry by the standard charge anti-correlation requirement $q_\mu \cdot q_\pi < 0$.
- The reconstruction efficiency strongly depends on VPDL [6], which can change the result of the integration in (4). Possible efficiency effects were investigated taking the efficiency model for $B_s^0 \to D_s^- \mu^+ \nu X$ decay from [6]. No sizable effect was found.

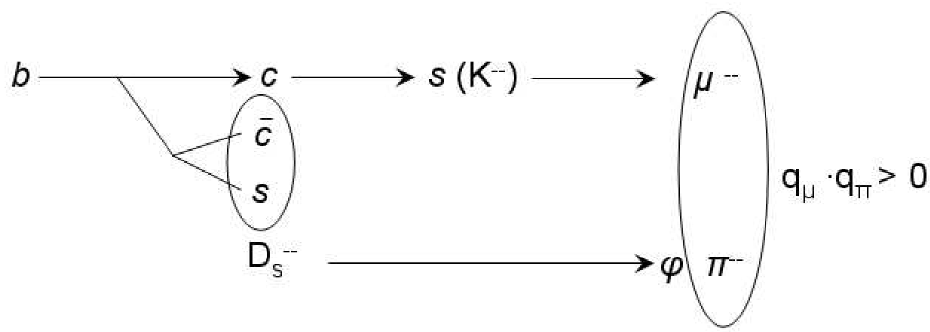

FIG. 2: Rejection of $K^\pm \to \mu^\pm$ events by the $q_\mu \cdot q_\pi < 0$ requirement.

The following sources of systematic errors were considered essential, their contributions multiplied by a factor of 2 according to (6), divided by the signal contribution (83.2%) where necessary, and added up in quadrature. A summary is presented in Table VII.

- Different interaction of π^+ and π^- with the detector material.

In selecting our signal we rely on pions. A pion may escape undetected if it interacts with the detector material inside the SMT. PDG sources [15] report different interaction cross-sections for π^- and π^+ with matter, in the range $1-2$ GeV: $\sigma(\pi^- d)$ is larger then $\sigma(\pi^+ d)$ by 1.3 ± 0.3 %. So π^+-s of $1-2$ GeV are more likely to be detected, which induces an asymmetry.

We assume that the SMT material crossed by a particle on its way out is equivalent to 2 cm of bulk beryllium (this is likely to be an overestimate). Taking the nuclear interaction length of beryllium from [11] we calculate that approximately 2% of pions get lost in the SMT. This induces an asymmetry $< 0.02 \cdot 0.01 = 2 \cdot 10^{-4}$ which contributes to the systematic error of the measurement.

- Error on the sample composition.

  This error was calculated by varying the signal contribution ($83.2 \pm 3.3\%$) by one standard deviation. It accounts for any variations of the signal fraction between different $\beta\gamma q$ subsamples, which we expect to be negligible. For instance, we studied relative fractions of the signal process $B_s^0 \to \mu^+\nu D_s^-$ and the most significant background process $B^0 \to D^+ D_s^- X; D \to \mu\nu X$ on Monte Carlo separately for $\eta_\mu > 0$ and $\eta_\mu < 0$. Both Monte Carlo samples were applied the same selection cuts we used to select data. We then fitted $M(KK\pi)$ distribution with a double Gaussian separately for positive and negative η_μ, and extracted the number of events in the D_s mass peak. The number of events and their ratios which represent the relative fractions of two chosen Monte Carlo processes are shown in Table VI. Clearly, the relative fraction does not depend on η_μ. This justifies the way we account for the sample composition by dividing the muon charge asymmetry by the signal contribution and introducing a systematic error from the sample compostition uncertainty.

TABLE VI: Number of events in D_s mass peaks of two Monte Carlo samples and their ratio which estimates the relative fraction of the chosen processes.

	$B_s^0 \to \mu^+\nu D_s^-$	$B^0 \to D^+ D_s^- X; D \to \mu\nu X$	*relativefraction*
$\eta_\mu > 0$	5332 ± 74	1690 ± 41	3.15 ± 0.09
$\eta_\mu < 0$	5318 ± 74	1678 ± 41	3.17 ± 0.09

- Mass fitting.

  The systematic error from the mass fitting procedure was calculated by varying the background slope and widths of D^- and D_s^- peaks by one standard deviation. We also repeated the mass fitting procedure with a single Gaussian describing the signal D_s^- peak and varied the fitting range. For any combination of variations the systematic error does not exceed $0.12 \cdot 10^{-2}$.

- A_{SL}^d contribution to the muon charge asymmetry.

  The effect of A_{SL}^d is accounted for as a systematic error and does not contribute more then $0.01 \cdot 10^{-2}$.

In conclusion, the total systematic error is $\Delta A_{SL}^s = 0.35 \times 10^{-2}$.

TABLE VII: Systematic errors of A_{SL}^s.

Source of error	ΔA_{SL}^s, $\times 10^{-2}$
Different interaction of π^+ and π^- with SMT material	0.02
Sample composition	0.10
Mass fitting	0.12
A_{SL}^d contribution to muon charge asymmetry	0.01
Total	0.35

VII. RESULT AND CONCLUSIONS

Using an untagged sample of $B_s^0 \to D_s^- \mu^+ \nu X$ decays, where $D_s^- \to \phi\pi^-$, $\phi \to K^+K^-$ we performed a measurement of the semileptonic decay rate asymmetry. Our final result is

$$A^s_{SL} = [2.45 \pm 1.93(\text{stat}) \pm 0.35(\text{syst})] \times 10^{-2},$$

which is the first direct measurement of A^s_{SL}. The error is dominated by statistics, so the result can be improved after a larger sample is available or additional processes are included in the signal.

---

[1] Yuval Grossman *et al*, Constraining the Phase of $B_s - \overline{B}_s$ Mixing, [arXiv:hep-ph/0605028 v2]

[2] Ulrich Nierste, CP asymmetry in flavor-specific B decays, [arXiv:hep-ph/0406300 v1]

[3] K.Anikeev *et al*, B Physics at Tevatron, Run II and Beyond, [arXiv:hep-ph/0201071]

[4] U. Nierste, Theory prediction for $\Delta\Gamma$ and $\Delta\Gamma/\Delta M$ in the B_s system, presentation at Chicago Flavor seminar, Fermilab, March 2006

[5] V.Abazov *et al*, The Upgraded DØ detector, [arXiv:hep-physics/0507191]

[6] C. Ay *et al*, B_s mixing in Semileptonic B^0_s decays Using the D_s to $\phi\pi$ Decay Mode and Unbinned Fit, DØnote 5017

[7] C. Ay *et al*, $c\overline{c}$ Contribution to $B_s \to D_s(\phi\pi)\mu\nu_\mu$ decay, DØnote 4639

[8] Lisa Randall and Shufnag Shu, CP Violating Lepton Asymmetries from B Decays and Their Implication for Supersymmetric Flavor Models, CERN-TH/98-159, [arXiv:hep-ph/9807377]

[9] D. J. Lange, NIM A 462 (2001) 152; for details see http://www.slac.stanford.edu/ lange/EvtGen

[10] The DØ collaboration, A Study of B^0_s oscillations, DØnote 5045

[11] S. Eidelman *et al*, Phys. Lett. **B592**, 1 (2004)

[12] The DØ collaboration, B_d mixing measurement using Opposite-side Flavor Tagging, DØnote 5029

[13] B.Hoeneisen, Measurement of CP-violation parameter of the (B^0, $\overline{B}^0$) system using 970 pb^{-1} of data, DØnote 4996

[14] F.James, MINUIT - Function Minimization and Error Analysis, CERN Program Library Long Writeup D506, 1998

[15] Carter *et al*, Pion-Nucleon Total Cross Section from 0.5 to 2.65 GeV/c, Physicsal Review, Vol. 168, Num. 5, 25 April 1968

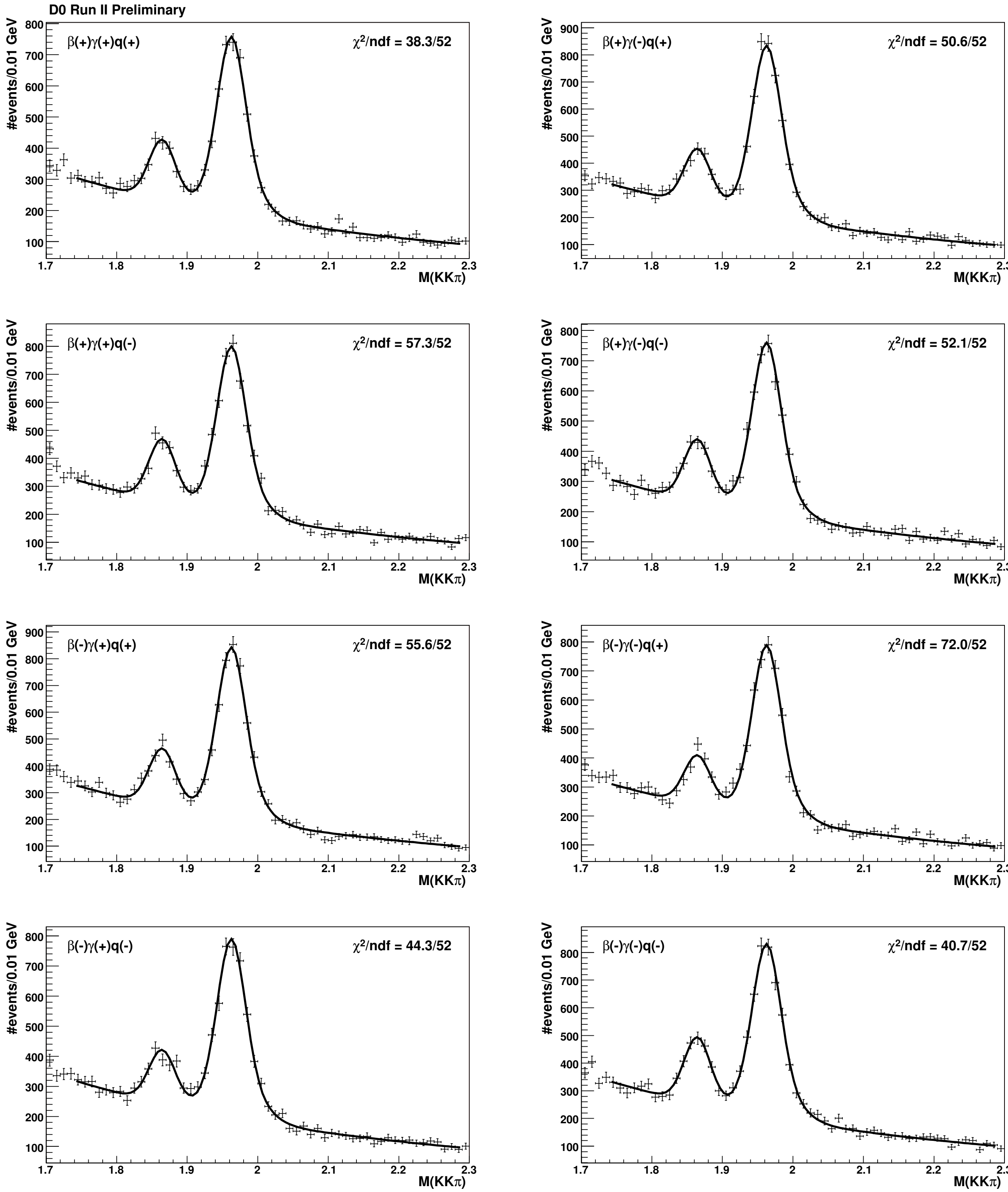

FIG. 3: $M(KK\pi)$ invariant mass distribution of the B_s^0 subsamples corresponding to 8 possible combinations of $\beta\gamma q$. The fit using the sum of a single Gaussian for the D^- mass peak, a double Gaussian for the signal D_s^- mass peak and an exponential for the background is also shown. During the fitting procedure the mass peak widths, positions, the fraction of a "second" Gaussian in the D_s^- peak and the background slope of the $M(KK\pi)$ distribution of every subsample were fixed to the values defined from the $M(KK\pi)$ fit of the undivided sample.